R-823

MICROSTRUCTURE AND THERMAL CONDUCTIVITY OF LAYERED THERMAL BARRIER COATINGS PROCESSED BY PLASMA SPRAY AND PHYSICAL VAPOR DEPOSITION TECHNIQUES

K. S. Ravichandran, K. An, R. E. Dutton* and S. L. Semiatin*
Department of Metallurgical Engineering
412 WBB, University of Utah, Salt Lake City, UT 84112, USA
*Materials Directorate, WL/MLLM, Wright Laboratory
Wright Patterson Air Force Base, OH 45433, USA

SUMMARY

Thermal conductivity is an important design parameter for thermal barrier coatings. Accurate thermal conductivity data is therefore required to ensure proper design and reliability of gas turbine blades. In the present research, thermal conductivities of Al_2O_3 and 8wt.% Y_2O_3 stabilized ZrO_2 (8YSZ) coatings, including monolithic and multilayer configurations, made by air plasma spray (PS) and electron beam physical vapor deposition (EB-PVD) techniques, were determined from the measurements of thermal diffusivity and specific heat as a function of temperature. Thermal diffusivity was determined by the laser flash technique. Specific heat was determined by a Differential Scanning Calorimeter (DSC). Detailed analyses of the results indicate that in the case of PS coatings, the thermal conductivity is sensitive to coating density (porosity), interfaces between splats as well as the interface between the coating and the substrate. In the case of EB-PVD coatings, it is shown that the multilayer conductivity is simply a series representation of monolithic coatings, provided comparisons are made under same microstructural condition. Further, analyses of sensitivity of the laser flash technique to variations in the coating and the substrate parameters, for the coatings evaluated in this study, were also performed. The results are discussed in the context of coating characteristics, reference conductivity data for dense materials and the sensitivity of the measurement method to coating parameters.

1. INTRODUCTION

High temperature materials are often protected by the use of thermal barrier coatings (TBCs) [1-4]. These coatings are applied by plasma spray (PS) or electron beam physical vapor deposition (EB-PVD) techniques with an intermediate NiCoCrAlY alloy bond coating to improve adherence and to reduce oxidation. The principal TBC material is Zirconia (ZrO_2) partially stabilized with about 6 to 8 wt.% Y_2O_3 (hereafter referred to as "YSZ"; for example, 8YSZ is used to refer to ZrO_2 stabilized with 8wt.% Y_2O_3. Hereafter, the composition of Y_2O_3 is quoted in wt.%, unless otherwise indicated) owing to its reasonable toughness (due to transformation toughening), low density, low thermal conductivity, high melting point, and good thermal shock resistance.

Although YSZ has low thermal conductivity, yet further reductions in thermal conductivity are caused by porosity and thermal resistance at imperfect interfaces in the coating. However, there has been limited work [5-9] performed to generate an understanding of the coating aspects that influence the heat transfer characteristics. Additionally, the conductivity data reported in the literature exhibit significant variations due to differences in processing parameters and microstructural characteristics. Among the microstructural variables that are known to have an effect on thermal conductivity, only the effects of the type and the amount of stabilizer in ZrO_2 has been studied in a systematic fashion [5, 7, 8]. Further, microstructural differences between bulk Al_2O_3 and YSZ and the coatings often exacerbates the difficulty in the assessment of coating thermal conductivity.

The primary objective of this study was to understand the issues involved in the assessment of thermal conductivity of Al_2O_3 and YSZ made by PS and EB-PVD techniques. For this purpose, thermal conductivity of coatings were studied from room temperature to 1000°C. The results are analyzed in terms of: (i) coating porosity, (ii) thermal resistance at the interfaces, (iii) the discrepancy among the thermal conductivity data of monolithic materials and (iv) the coating microstructure relative to that of the dense materials. The

Paper presented at an AGARD SMP Meeting on "Thermal Barrier Coatings", held in Aalborg, Denmark, 15-16 October 1997, and published in R-823.

reliability of the conductivity data is assessed in terms of the sensitivity of the laser flash technique to the uncertainties in the coating and the substrate parameters.

2. EXPERIMENTAL PROCEDURE

Plasma-sprayed coatings were obtained by spraying 8YSZ and Al_2O_3 onto 3 mm thick Rene 95 superalloy substrates measuring 62.5 mm X 12.5 mm. Prior to deposition, the substrate surfaces were grit blasted to improve coating adherence. Powders of 8YSZ (Metco 204NS; average particle size: 10 μm) and Al_2O_3 (Plasmalloy Al-1010; average particle size: 5 μm) were used. A Plasma Technik Spray system with a single spray nozzle and dual powder feeder was employed. Both monolithic and multilayer coatings involving alternating layers of Al_2O_3 and 8YSZ were prepared. The coatings exhibited residual porosity. Porosity levels were determined using measurements of coating mass and volume as well as by image analysis and point counting techniques on optical micrographs. To determine if residual porosity could be closed by sintering, heat treatment of the coatings was performed at 1300°C for 50 hrs in a furnace under flowing argon. For this purpose, 10 mm^2 size samples, cut using a diamond wafering blade, were employed. The coatings detached from the substrate as units after the heat treatment. The surfaces of the detached coatings that corresponded to the coating-substrate interfaces were metallographically polished to remove the metal oxide layers formed during the heat treatment. EB-PVD coatings were made by electron beam evaporation of high purity Al_2O_3 and 8YSZ sputtering targets on to CMSX-4 single crystal superalloy substrates. The substrate temperature was about 300-500°C during the deposition process. Both monolithic and multilayer coatings involving alternating layers of Al_2O_3 and 8YSZ were prepared by this technique.

Thermal diffusivity measurements were made using the laser flash technique [10]. The laser flash technique involves heating one side of the sample with a laser pulse of short duration and measuring the temperature rise on the other side with an infrared detector. The thermal diffusivity is determined from the time required to reach one-half of the peak temperature and a transient heat conduction analysis of a two-layer body. From this analysis, the thermal diffusivity of a single layer coating on a substrate can be independently determined. Measurements were made on the coatings with substrate in the as-sprayed condition and on the detached coatings in the heat-treated condition. Measurements were made from room temperature to a temperature of 1000°C. For the high temperature measurements, the samples were heated in a vacuum chamber in 100°C steps; a thermal diffusivity measurement was made at each step. Specific heat measurements of Al_2O_3 and 8YSZ were also made using a standard Perkin-Elmer Model DSC-2 Differential Scanning Calorimeter with sapphire as the reference material. Powders, scrapped from the as-sprayed coatings were used for this purpose. The standard and the sample were subjected to the same heat flux as a blank and the differential powers required to heat the sample and standard at the same rate were determined. From the masses of the sapphire standard and the sample, the differential power, and the known specific heat of sapphire, the specific heat of the sample was computed. The thermal conductivities of the coatings were determined using the relationship:

$$k = \alpha C_p \rho \qquad \ldots(1)$$

in which k is the thermal conductivity, α is the thermal diffusivity, C_p is the specific heat and ρ is the density of the coating. X-ray diffraction analyses of the coatings were performed using Siemens D5000 unit, with CuKα radiation, to identify the phases.

3. RESULTS: PLASMA SPRAYED COATINGS

(a) Monolithic Coatings:

Microstructures of the as-plasma sprayed coatings are shown in Fig. 1(a&b); those after heat treatment are illustrated in Fig. 2(a&b). The coatings exhibited a porous structure, typical of air-plasma-sprayed TBCs. A comparison of Figures 1 and 2 reveals little change in porosity in Al_2O_3 and YSZ layers after heat treatment. Therefore, porosity levels in the as-sprayed condition were assumed for the heat treated coatings.

Table I. Data on Monolithic Coatings

Property	Al_2O_3	8YSZ
Coating thickness (mm)	0.34	0.37
Porosity (%)	19	12
Density of monolithic (g/cc)	3.9	5.74
Expt. coating density (g/cc)	3.17	5.06
Calc. coating density (g/cc)	3.28	5.13

The porosity, density and the thickness of each coating are presented in Table I. As mentioned above, porosity levels were determined by a "mass/volume" (direct) measurement, or by

Fig. 1(a) Microstructure of PS Al_2O_3 in the as-sprayed condition

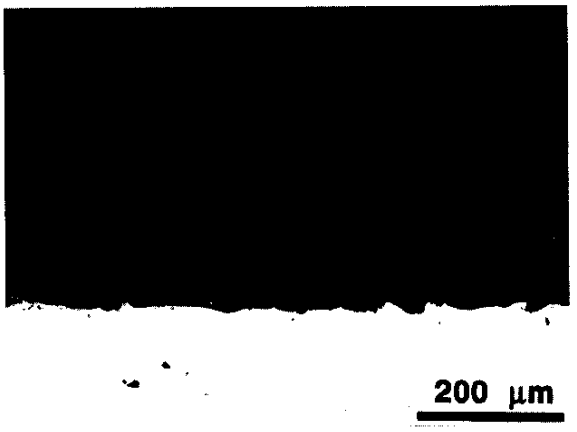

Fig. 1(b) Microstructure of PS 8YSZ coating in the as-sprayed condition

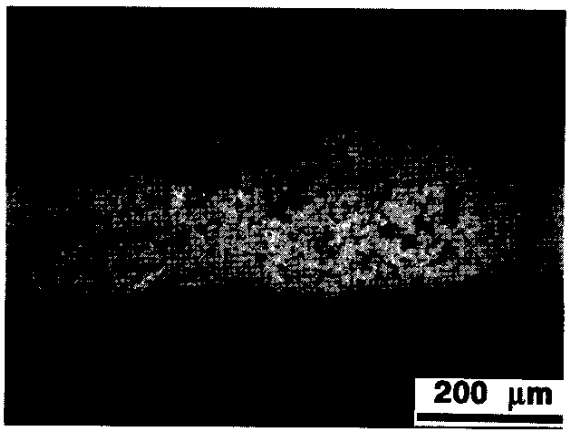

Fig. 2(a) Microstructure of PS Al_2O_3 in the heat treated condition

image analysis/point counting techniques on polished cross-sections. The various techniques gave reasonable agreement once polishing procedures were optimized to minimize particle pull-out. Additionally, the density values determined using the porosity levels in Table I and the theoretical densities were nearly in agreement, suggesting that the density values determined by the "mass/volume" technique are reliable.

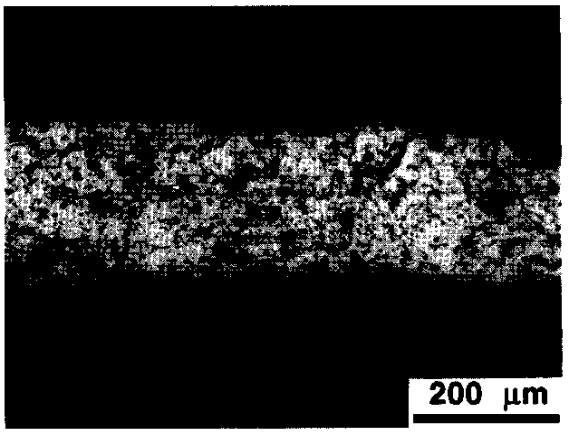

Fig. 2(b) Microstructure of PS 8YSZ in the heat treated condition

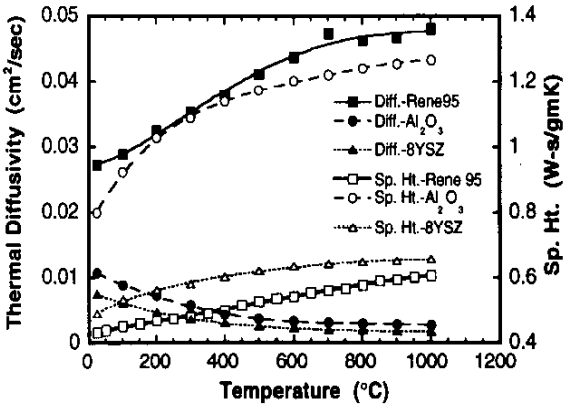

Fig. 3. Thermal diffusivity and specific heat data for Rene 95 substrate, Al_2O_3 and 8YSZ

Thermal diffusivity and specific heat data for the Rene 95 substrate, Al_2O_3 and 8YSZ are presented in Fig. 3. Thermal conductivities of monolithic Al_2O_3 and 8YSZ as-sprayed coatings as a function of temperature, determined through Eqn. (1) using the data in Fig. 3, are presented in Figures 4 and 5, respectively. In these figures, thermal conductivity of as-sprayed coatings are compared with that of the solid materials incorporating the effect of porosity. It is to be noted that that the data for solid Al_2O_3 could not be obtained during the period of this study, due to difficulties in sintering the spray powder. Therefore, the thermal

conductivity data reported in literature is employed in Fig. 4.

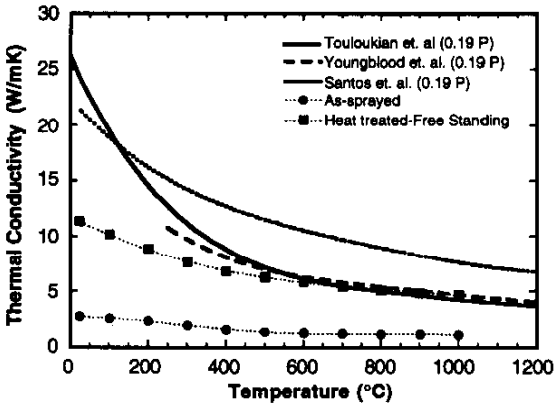

Fig. 4. Thermal conductivity of Al_2O_3 coatings compared with the porosity-corrected data for various solid Al_2O_3 reported in literature

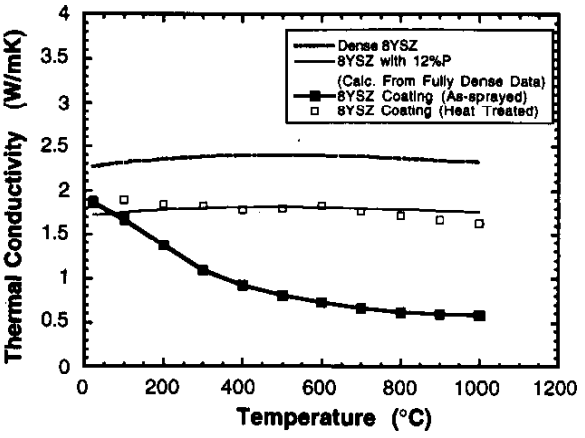

Fig. 5. Thermal conductivity of 8YSZ coatings compared with the porosity-corrected data of solid 8YSZ

The degree of reduction in thermal conductivity due to porosity can be calculated from [11]

$$k_p = k\left[1-P^{2/3}\right] \qquad ..(2)$$

in which k_p and k are the thermal conductivities of the porous material (with a porosity of volume fraction P) and the fully dense material, respectively. During the present work, Eqn. (2) was found to accurately describe the reduction in room-temperature thermal conductivity due to the presence of pores in solid Al_2O_3 and ZrO_2 ceramics, when evaluated [11] against the data on sintered monolithic materials reported in literature [12-15]. Therefore, Eqn. (2) was used to incorporate the effects of porosity on thermal conductivity in Figures 4 and 5.

(b) Multilayer Coatings

Microstructures of multilayer coatings: AZ4 and AZ8 are shown in Figs. 6 (a&b) in the as-sprayed condition and in Figs. 7 (a&b) after heat treatment. A refers to Al_2O_3 and Z refers to 8YSZ, with the numbers indicating the number of layers of each material. For example, AZ4 contains 4 layers of Al_2O_3 and 4 layers of 8YSZ, arranged alternatingly. Table II illustrates the total coating thickness, individual layer size and the experimentally measured and calculated porosity levels, for various multilayer coatings made by the PS technique.

Fig. 6(a) Microstructure of PS AZ4 coating in the as-sprayed condition

Fig. 6(b) Microstructure of PS AZ8 coating in the as-sprayed condition

Thermal conductivity data as a function of temperature for multilayer coatings in the as-sprayed and sprayed-and-heat treated conditions are presented in Figures 8 and 9, respectively. The conductivity data for fully dense materials are also included. In addition, estimates of conductivity of bilayer coatings (assuming Al_2O_3 and 8YSZ in series) using either the porosity-corrected data for fully dense Al_2O_3 and 8YSZ or

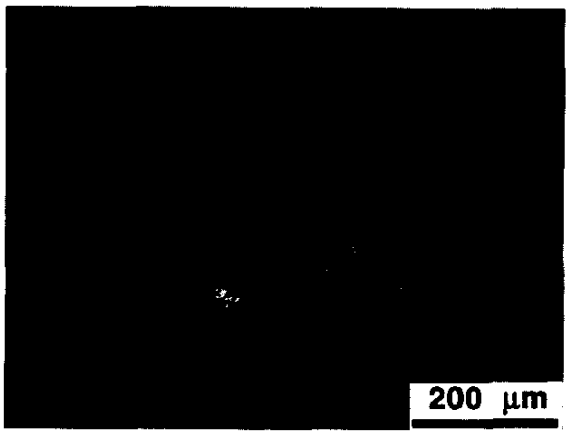

Fig. 7(a) Microstructure of PS AZ4 coating in the heat treated condition

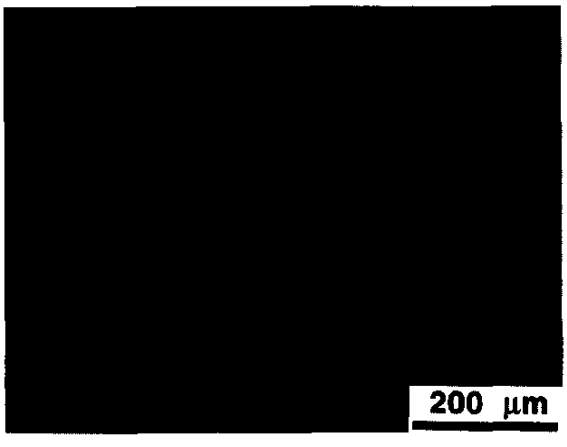

Fig. 7(b) Microstructure of PS AZ8 coating in the heat treated condition

Table II. Data on Multilayer Coatings

Property	AZ1	AZ2	AZ4	AZ8
Thickness (mm)	0.36	0.36	0.35	0.35
Each layer size (mm)	0.18	0.09	0.044	0.022
Porosity (%)	15.5	17	12.7	13.7
Density of solid (g/cc)	4.82	4.82	4.82	4.82
Coating density* (g/cc)	4.07	4.0	4.21	4.16
Coating density^{+} (g/cc)	4.17	4.12	4.28	4.24

*Experimentally determined

$^{+}$Calculated from porosity and solid density

the experimentally measured data for monolithic Al_2O_3 and 8YSZ coatings, are presented. These calculations were performed using Equation (3) in the following form:

$$k_c = \frac{k_a k_z}{(k_a t_z + k_z t_a)} \qquad ...(3)$$

in which k_c is the composite thermal conductivity with the layers in series arrangement, and t_a and t_z are the thickness fractions of Al_2O_3 and 8YSZ layers, respectively. Because the thickness fractions of Al_2O_3 and YSZ are nearly the same and equal in all of the multilayer coatings, these calculations provide a baseline for comparison with the measured thermal conductivities of the multilayer coatings.

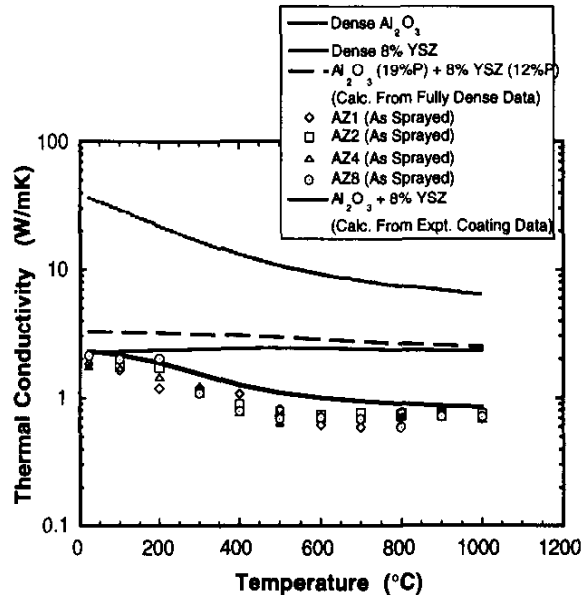

Fig. 8. Comparison of experimental conductivity data of as-sprayed multilayers with the data for monolithic dense materials as well as calculated data for a bilayer coating

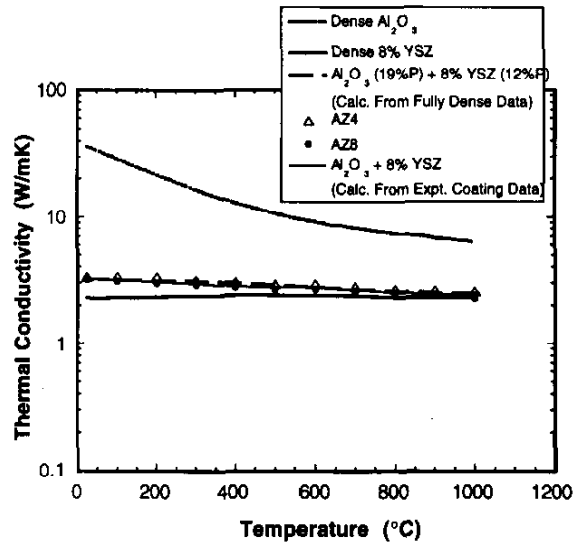

Fig. 9. Comparison of experimental conductivity data of heat treated multilayer coatings with the data for monolithic dense materials as well as calculated data for a bilayer coating

4. DISCUSSION: PLASMA SPRAYED COATINGS

(a) Monolithic Coatings:

The conductivity levels in the as-sprayed condition are substantially lower than the porosity-incorporated data of solid materials, for both Al_2O_3 and 8YSZ coatings (Figs. 4 & 5). However, the data of Al_2O_3 and 8YSZ free-standing heat treated coatings agreed well with the porosity-incorporated data of solid materials. For Al_2O_3, the agreement is good with the data of Youngblood et. al. [16]. The rationale behind this choice is discussed in the next section.

The heat treated coatings differed from the as-sprayed in two respects: (i) a high degree of elimination of interfaces between the splats in the coating due to sintering and (ii) the elimination of the coating/substrate interface, since the coatings detached after heat treatment. Therefore, the increase in conductivity is perceived to be due to the elimination of both of these interfaces in the heat treated condition.

Since dense specimens of Al_2O_3, for reference conductivity measurements, could not be made from the plasma spray powders, conductivity data reported in literature for Al_2O_3 were used in assessing the conductivities of present coatings. In this context, one of the primary issues is the accuracy of reference data and the equivalency of the microstructure of the reference material to that of the coating. For example, the literature thermal conductivity data (Fig. 4) for solid Al_2O_3 differed significantly, possibly due to variations in microstructure. The data of Youngblood et. al. [16] was generated using AD 995 Al_2O_3 powder (Coors Ceramics, Inc., Golden, CO.) sintered to >99% theoretical density. The details regarding purity, phases and microstructure were not available. The data of Touloukian et. al. [17] is for Al_2O_3 having >98% theoretical density, but the details on purity and phases were not available. The data of Santos et. al. [18] was generated using 99.8% pure Al_2O_3 (A-16SG powder from ALCOA) and correcting the measured conductivity data for residual porosity. Because of the different sources of these powders, considerable variability in the thermal conductivity data of dense Al_2O_3 is seen (Fig. 4). Further, since the details on purity, phases and microstructure are not known, a comparison of them with the Al_2O_3 coating is difficult. The X-ray diffraction pattern of the Al_2O_3 coating is shown in Fig. 10. The figure indicates that both α-Al_2O_3 and γ-Al_2O_3 phases are present in significant quantities. In addition, small intensity maxima, characteristic of an amorphous phase, such as SiO_2, are also present. Amorphous SiO_2 is known [19] to be present as grain boundary phase in sintered Al_2O_3. Due to its low thermal conductivity relative to Al_2O_3, a significant change in conductivity, due to small changes in SiO_2 content can be expected. Figure 4 indicates that the conductivity data of Youngblood et. al. [16] agreed better with that of the heat treated material. The lack of agreement with the data of other reference materials, even after correcting for porosity, could be due to the microstructural differences between the coating and these materials. Further study is needed to clarify the role of purity, phases and microstructure on the thermal conductivity of Al_2O_3.

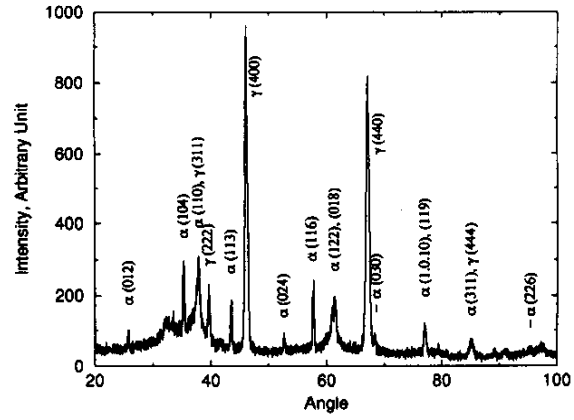

Fig. 10. X-ray diffraction pattern for as-sprayed Al_2O_3 coating.

(b) Multilayer Coatings:

Figure 8 reveals that the thermal conductivities calculated from Equation (3), using the data for dense materials and accounting for porosity, are significantly higher than the experimental measurements for the multilayers. On the other hand, the estimates from Equation (3) using the experimental conductivity data for the monolithic Al_2O_3 and 8YSZ coatings are in reasonable agreement with the multilayer data. The latter agreement may be surmised to be due to the effect of thermal resistance due to splat interfaces and cracks, which is already included in the conductivities of the monolithic coatings. The conductivities of all of the multilayer coatings fall in a narrow band, suggesting that the contribution from the interlayer interfaces in reducing the overall thermal conductivity of the coating is relatively small. It should be noted that all the coatings had the same overall thickness with varying number of layers and corresponding layer thicknesses. Therefore, the

total number of splat interfaces in each coating can be expected to be nearly the same. It appears that due to this similarity, the thermal conductivity levels of multilayer coatings differed little and thus can be predicted with reasonable accuracy from the experimental data of monolithic coatings.

While the measured conductivity data for all the as-sprayed multilayer coatings showed a significant decrease with temperature, the data after heat treatment (Figure 9) were largely independent of temperature. Several microstructural factors should be considered in understanding thermal conductivity changes after heat treatment. Porosity and thermal resistance at interfaces can significantly influence the thermal conductivity in solids [4, 5, 10, 11, 15]. Since porosity levels changed only a little, the effect on thermal conductivity due to this change can be considered negligible. On the other hand, interfaces between the splats in thermal sprayed coatings have been suggested to reduce the thermal conductivity due to the interface thermal resistance [5, 11]. This effect due to internal interfaces can be appreciated from the data shown in Fig. 9. The predictions for a bilayer, calculated from the porosity-corrected data of fully dense materials as well as from the experimental data for heat-treated monolithic coatings using Equation (3), agree well with the experimental data for multilayer coatings. This suggests that heat treatment may have eliminated the effects due to the imperfect splat interfaces in the coatings and that the primary microstructural factor that influences thermal conductivity in this condition is the porosity within the layers. However, since the coatings detached after heat treatment, it was not possible to determine the relative contribution of the coating-substrate interface versus that of the splat interfaces.

5. RESULTS: EB-PVD COATINGS

Details of EB-PVD coatings, including total coating thickness, individual layer thickness and density are presented in Table III.

Table III. Description of Coatings, Layer Thickness and Density Values for EB-PVD Coatings with CMSX Single Crystal Substrates.

ID	Coating Type	Calc. Density* (gm/cc)	Meas. Density (gm/cc)	Subst. Thick. (mm)	Total Coating Thick. (mm)	Thick. of 8YSZ layer (mm)	Thick. of Al_2O_3 layer (mm)
PVD2	Substrate+ bond coat**	8.567	8.52	0.915***			
PVD4	PVD2 + 1 layer 8YSZ	5.74	5.41	0.865	0.111	0.111	
PVD5	PVD2 + 1 layer each of Al_2O_3 and 8YSZ	4.75	4.69	0.749	0.094	0.049	0.045
PVD6	PVD2 + 4 layer each of Al_2O_3 and 8YSZ	4.65	4.71	0.609	0.116	0.015	0.014
PVD7	PVD2 + ≈ 350 alt. Al_2O_3 and 8YSZ layers	5.11	4.64	0.614	0.117	0.00065	0.00035
PVD8	PVD2 + ≈ 1000 alt. Al_2O_3 and 8YSZ layers	5.08	4.83	0.485	0.139	0.00064	0.00034

* Calculated from theoretical density of Al_2O_3 and 8YSZ, using layer thicknesses.
** Substrate+bond coat was treated as a single material in thermal conductivity measurements and calculations.
*** Refers to the total thickness of bond coat + substrate.

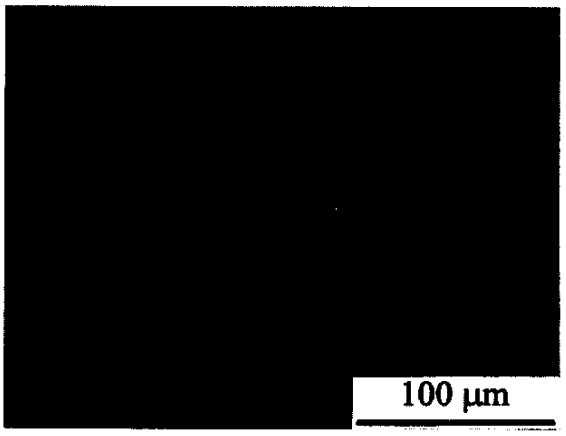

Fig. 11. Microstructure of single layer EB-PVD 8YSZ coating

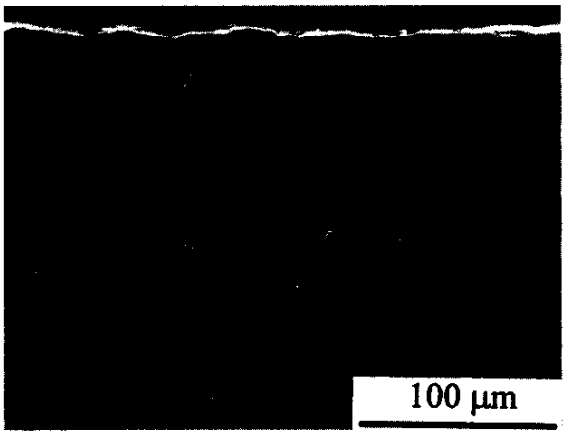

Fig. 12. Microstructure of multilayer coating with 4 alternating layers of each of 8YSZ and Al_2O_3

Microstructures of EB-PVD coatings are presented in Figs. 11 through 13. Figures 11 and 12 illustrate the microstructures of the single layer 8YSZ (PVD4) and 8 layer coating involving 4 alternate layers of each of 8YSZ and Al_2O_3, respectively. Figures 12 (a&b) illustrate the microstructure of the multilayer coating with about 350 total alternating layers of 8YSZ and Al_2O_3. The microstructure of single layer 8YSZ coating is an array of fairly closely packed columns that run perpendicular to the interface of coating and substrate. As the total number of layers was increased, the tendency to exhibit the columnar structure decreased. The measured thermal conductivity data as a function of temperature for all the coatings studied are presented in Fig. 14. The solid 8YSZ data is for the original bulk material that was used to deposit the coating. Al_2O_3 could not be sintered to obtain a dense material. Therefore, the data for solid Al_2O_3 was taken from literature. This data is the same (Santos et. al. [18]) as the data reported in Fig. 4. Additionally, single layer Al_2O_3 coating with the same thickness as the other coatings, could not be deposited without cracking and spallation. The data calculated on the basis of series heat transfer model (Eqn. 3) using the thickness fractions of layers in each type of coating, is also presented. It can be seen that the multilayers have higher conductivity that that of 8YSZ, but lower than the data of bulk Al_2O_3, as expected. It appears that as the columnar nature of the layers decreased, the thermal conductivity also decreased. This is clearly evident by comparing the data of 2 layer coating and the 8 layer coating.

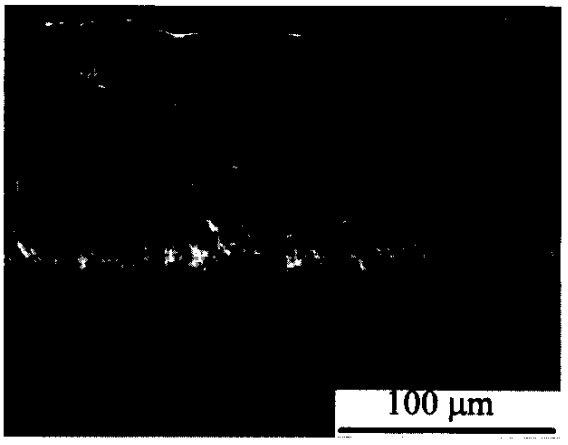

(a)

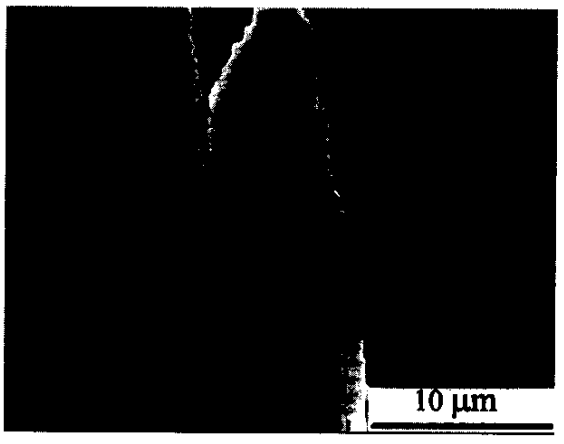

(b)

Fig. 13 (a&b). Microstructures of multilayer coating with 350 total alternating layers of 8YSZ and Al_2O_3

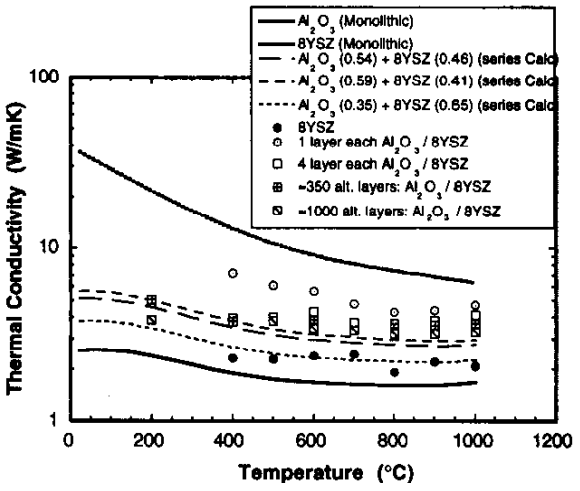

Fig. 14. A comparison of the experimental thermal conductivities of EB-PVD coatings with the data for solid materials and the calculated data for multilayer coatings

6. DISCUSSION: EB-PVD COATINGS

First of all, the thermal conductivity data of 8YSZ coating is higher than the bulk 8YSZ data by a factor of 1.5. In order to understand this discrepancy, some microstructural factors are to be considered. The solid 8YSZ and the coating deposited using it, were found to be not under the same microstructural condition. Whereas the solid consisted of a mixture of monoclinic and tetragonal phases (Fig. 15), the coating consisted almost entirely of tetragonal phase (Fig. 16). The type of phase present in the YSZ microstructure is known [20] to affect the thermal conductivity and therefore, this factor should be considered in the comparison of the monolithic material and the coating.

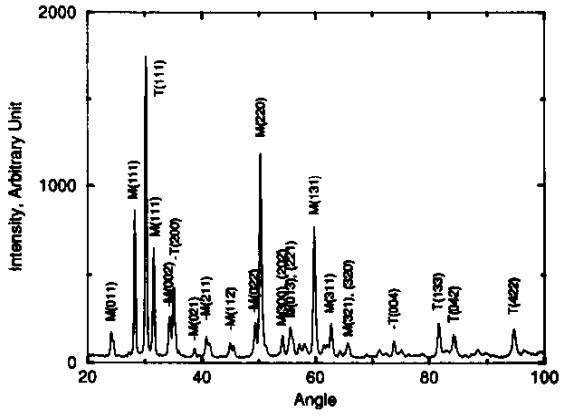

Fig. 15. X-ray diffraction pattern for solid 8YSZ material

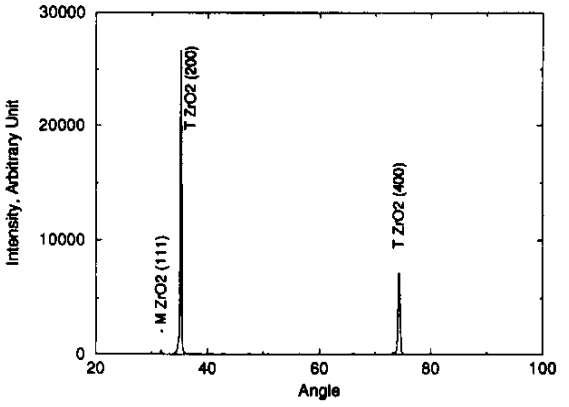

Fig. 16. X-ray diffraction pattern for the 8YSZ coating

First, it is of interest to see how the relative proportion of phases in YSZ, influenced by Y_2O_3 level, would influence the conductivity of YSZ. In Fig. 17, the conductivity data of various dense YSZ specimens reported in literature [16,20,21], as well as that of solid 8YSZ evaluated in the present study, are compared. The data differed significantly among them, owing to the variation in the amount of Y_2O_3 stabilizer. For example, increasing Y_2O_3 from 5.3wt.% to 9wt.%, a significant decrease in the conductivity level can be seen, over the entire temperature range. However, at 11wt.% Y_2O_3, the conductivity appears to increase, relative to that of 8-9wt.% Y_2O_3 stabilized ZrO_2 specimens. This trend is consistent with the variation in thermal diffusivity as a function of Y_2O_3 content, as observed by Youngblood et. al. [16].

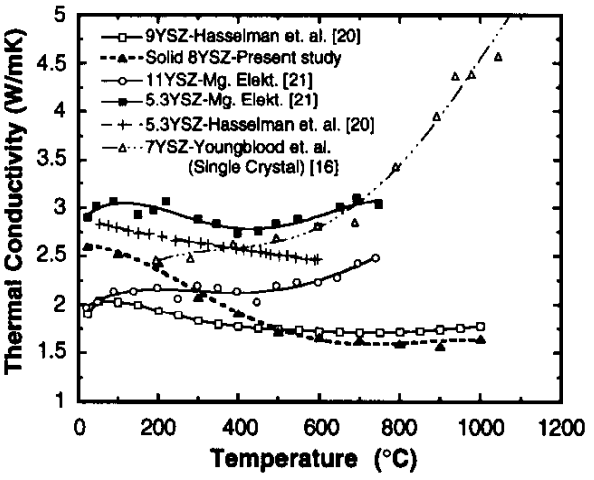

Fig. 17. Thermal conductivity data for YSZ with various amount of stabilizer content, compiled from literature

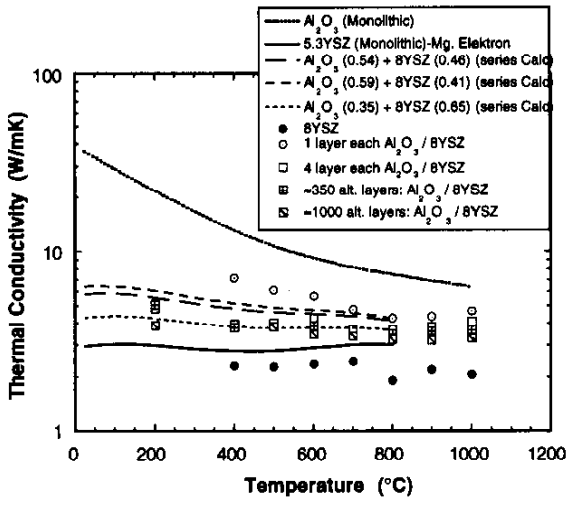

Fig. 18. A comparison of the experimental thermal conductivities of EB-PVD coatings with the revised data

The study of Hasselman et. al [20] indicates that in the range of Y_2O_3 content varying from 4.5 to 5.5 wt.%, Y_2O_3, YSZ almost entirely consists of tetragonal phase. Above 5.5 wt.% Y_2O_3, a mixture of tetragonal and monoclinic phases was seen. The proportion of monoclinic phase was determined to be 25% in the 8.6YSZ specimen. This is consistent with the X-ray data of 8YSZ dense material (Fig. 15) evaluated in the present study. Therefore, the present 8YSZ coating and the 8YSZ dense material are not truly comparable due to the differences in the amount of tetragonal and monoclinic phases. The relative proportions of phases can affect the thermal conductivity of coatings due to: (i) the second phase-effect on thermal conductivity in composites [19], (ii) phonon scattering at the interphase interfaces [22] and (iii) a change in defect structure with composition [23]. In Fig. 18, the thermal conductivity comparisons employed in Fig. 14 have been revised using the solid 5.3wt% YSZ conductivity data, since, this material entirely consisted of tetragonal phase. As can be seen, the agreement between the conductivities of solid 8YSZ and 8YSZ coating as well as between the experimental data and the calculated data for multilayer coatings has improved. It is to be noted that the variations between the conductivity levels of multilayer coatings appear to be due to differences in the relative layer thicknesses of 8YSZ and Al2O3 layers.

7. ANALYSIS OF SENSITIVITY OF THERMAL CONDUCTIVITY MEASUREMENT

Thermal diffusivities of the coatings with the substrate, investigated in this study, were determined using a two-layer calculation procedure which is discussed in detail elsewhere [10]. The input parameters which enter this calculation are the thicknesses, densities and the specific heat values of the coating and the substrate, the thermal diffusivity of substrate and the measured half-times. The sensitivity of each of these parameters also depends on the relative values between these parameters, i.e. the relative layer thicknesses, the relative magnitudes of diffusivities, etc. The situation is further complicated by the fact that the calculation of the diffusivity (or conductivity) of the coating is an iterative procedure. The effect of uncertainties in the input parameters for the PS and EB-PVD 8YSZ coatings, on their calculated thermal conductivity values, was determined by introducing positive and negative errors in the parameters. The changes in the coating conductivity values are plotted as a function of positive and negative changes in different input parameters, in Figs. 19 and 20 for 8YSZ coatings, deposited by PS and EB-PVD techniques, respectively.

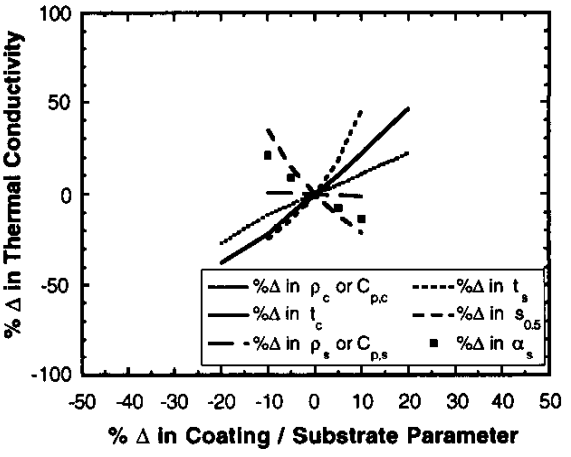

Fig. 19. Sensitivity of thermal conductivity of PS 8YSZ coating to the changes in coating/substrate parameters

For the PS 8YSZ coating, in the order of decreasing sensitivity, the coating conductivity is sensitive to: substrate thickness (t_s), half-time ($S_{0.5}$), substrate diffusivity (α_s), coating thickness (t_c), coating density (ρ_c) or specific heat ($C_{p,c}$) and substrate density (ρ_s) or specific heat ($C_{p,s}$). For example, for PS 8YSZ coating (Fig. 19), a -10/+10 change in the parameter caused changes in the coating conductivity as: -24/+46 for substrate thickness, +35/-20 for half-time, +22/-13 for substrate diffusivity, -21/+21 for coating

thickness, -11/+11 for coating density or specific heat and +1/-1 for substrate density or specific heat.

For the present PS coatings, the accuracy of the conductivity data principally depends on the parameters that cause the most variability in the present coatings. Since substrate thickness could be measured to the accuracy of 0.1 mm, the uncertainty in substrate thickness (0.03%) is too small to cause any change in coating conductivity. The half-times are recorded using digital oscilloscopes, so the uncertainty in their measurement can be considered to be better than 1%. The substrate diffusivity was independently measured using the free-standing sample and hence the measurements can be considered accurate within ±1%. The density of the substrate were determined within ±1% using the Archimedes principle. The specific heat values of the coating and the substrate can also be determined to a level of ±1% or better. This leaves the coating thickness and the density as the most sensitive parameters involved in the present study. The coatings thicknesses were of the order of 400 μm, with the coating surface roughness of the order of 40-50 μm, indicating that the variability in coating thickness is about 10%. Additionally, the measurements of density of plasma sprayed coatings could be in error to some degree, due to the penetration of liquid medium through the open pores. Therefore, the present thermal conductivity data for PS coatings can be expected to be subject to these uncertainties.

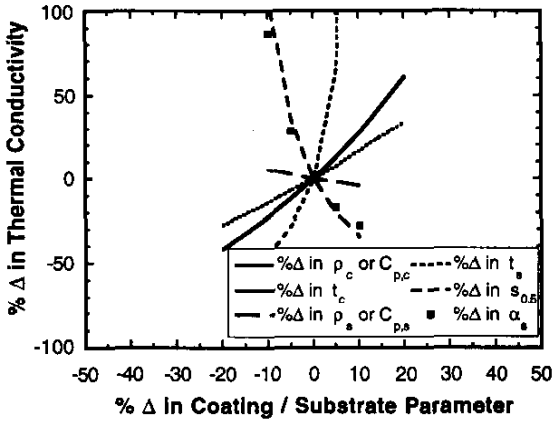

Fig. 20. Sensitivity of thermal conductivity of EB-PVD 8YSZ coating to the changes in coating/substrate parameters

For the EB-PVD coating, in the order of decreasing sensitivity, the coating conductivity is sensitive to: substrate thickness, half time, substrate diffusivity, coating thickness, coating density or specific heat and substrate density or specific heat. For example, a -10/+10 change in the parameter caused changes in the coating conductivity as: -44/+∞ for substrate thickness, +105/-35 for half-time, +86/-29 for substrate diffusivity, -22/+27 for coating thickness, -15/+16 for coating density or specific heat and +5/-3 for substrate density or specific heat (Fig. 20). The order of parameters in sensitivity ranking is similar to that of the PS coatings.

It is to be noted that for the EB-PVD coatings the variability encountered in coating parameters are about the same as that of the PS coatings. However, the EB-PVD coating thickness is a factor of 4 smaller compared to the PS coatings. The substrate thickness was 1 mm. The sample used for thermal conductivity measurement was prepared by mechanically grinding the substrate from its original thickness of 3 mm to 1 mm. After grinding, the average variation in substrate thickness was found to be about +/- 0.04 mm. This would suggest that the uncertainty in substrate thickness is +/-4%. Therefore, the increased sensitivity of conductivity data in the case of EB-PVD coating, relative to PS coatings, seems to arise from the reduced thicknesses of the coating and the substrate.

8. CONCLUSIONS

Plasma Sprayed Coatings:

(1) The reductions in the thermal conductivities of single layer as well as multilayer plasma-sprayed Al_2O_3 and 8YSZ coatings are brought about by porosity and thermal resistance at the interfaces in the coating. The thermal resistance appears to arise from the interfaces between the splats as well as the coating/substrate interface. The interlayer interfaces in the multilayer appears to play only a minor role in influencing the coating thermal conductivity.

(2) The thermal conductivity levels of multilayered coatings of Al_2O_3 and 8YSZ are comparable to that of the single layer 8YSZ coating. Therefore, primarily the interface thermal resistance and secondarily the porosity appear to be the parameters that can be manipulated to reduce the thermal conductivity of thermal barrier coatings.

(3) The uncertainty in the thermal conductivity values of the Al_2O_3 and ZrO_2 coatings were determined to be primarily due to the uncertainties in the coating thickness and density values.

EB-PVD Coatings:
(4) Microstructures of EB-PVD coatings consisted of an array of closely packed columnar grains. The columnarity decreased as the number of layers increased, in the case of multilayer coatings involving Al_2O_3 and 8YSZ.

(5) The Al_2O_3 and 8YSZ layers consisted of almost entirely γ-Al_2O_3 and tetragonal phase, respectively, in the coatings. This is in contrast to the observation of a mixture of α/γ phases in bulk Al_2O_3 and monoclinic and tetragonal phases in bulk 8YSZ.

(6) An accurate evaluation of thermal conductivity of EB-PVD coating requires accurate reference data on monolithic material having the same microstructural condition as the coating. For Al_2O_3, the relative proportion of α/γ phases, impurity levels and microstructure may influence the reference conductivity data. For YSZ, the nature and the proportion of phases appears to be important (tetragonal, cubic or monoclinic).

(7) Thermal conductivity of multilayer coatings can be predicted from the bulk material data, using the series heat transfer model. This suggests that there is no apparent effect of interface thermal resistance due to the interlayer boundaries.

(8) Thermal conductivity data determined by laser flash technique can be subject to considerable errors due to the variability in coating parameters that are used as input in the calculations. The errors increase as the coating and the substrate thicknesses become small.

ACKNOWLEDGMENT

The research at the University of Utah was supported by a contract (F33615-92-C-5900) from Wright Laboratory, Wright Patterson AFB, OH, through UES Inc., Dayton, OH. The authors thank Dr. S. Sampath, State University of New York, Stony Brook, NY, and Mr. K. Murphy, Operhall Research Center, Howmet Corporation for preparation of coatings and discussions.

REFERENCES

1. Miller, R. A., Surf. Coat. and Tech., 30, 1-11 (1987)
2. Lammermann, H. and Kienel, G., Adv. Mater. Processes, 140, 18-23 (1991)
3. Herman, H., Berndt, C. C. and Wang, H., Ceramic Films and Coatings, J. B. Wachtman and R. A. Haber, eds., 131-183, Noyes Publications, N. J. (1986)
4. Brink, R. C., Trans. ASME: J. Eng. for Gas Turbines and Power, 111, 570-577 (1989)
5. Pawlowski, L. and Fauchais, P., Int. Metall. Rev., 31, 271-289 (1992)
6. Pawlowski, L., Lombard, D. and Fauchais, P., J. Vac. Sci. Technol., 3, 2494-2500 (1985)
7. Brandon, J. R. and Taylor, R., Surf. Coat and Tech., 39/40, 143-151 (1989)
8. Morrell, P. and Taylor, R., in Advanced Ceramics, Vol. 24, Science and Technology of Zirconia, 927-943, The American Ceramic Society, Westerville, OH (1988)
9. Rudajevova, A., Thin Solid Films, 223, 248-252 (1993)
10. Taylor, R. E. and Maglic, K. D., Compendium of Thermophysical Property Measurement Methods, K. D. Maglic, ed., 305-336, Plenum Publishing Co., (1984)
11. Ravichandran, K. S., J. Am. Ceram. Soc., Submitted for Publication, (1997).
12. Francl, J. and Kingery, W. D., J. Am. Ceram. Soc., 37, 99-101 (1954)
13. Saegusa, T., Kamata, K., Iida, Y. and Wakao, N., Heat Transfer-Japanese Research, 3, 47-52 (1974)
14. Swain, M. V., Johnson, L. F., Syed, R and Hasselman, ., D. P. H., J. Mater. Sci. Lett., 5, 799-802 (1986)
15. Pei-feng Hsu and Howell, J. R., Expt. Heat Trans., 5, 293-313 (1992)
16. Youngblood, G. E., Rice, R. W. and Ingel, R. P., J. Am. Ceram. Soc., 71, 255-60 (1988)
17. Touloukian, Y. S., Powell, R. W., Ho, C.Y. and Clemens, P. G., Thermophysical Properties of Solids, 2, Y. S. Touloukian and C. Y. Ho, ed., Plenum Press, New York (1970)
18. Santos, W. N. D. and Taylor, R., High Temp.-High Press., 25, 89-98 (1993)
19. Kingery, W. D., Introduction to Ceramics, John-Wiley & Sons, New York (1967)
20. Hasselman, D. P. H., Johnson, L. F., Bentsen, L. D., Syed, R., Lee, H. M. and Swain, M. V., Am. Ceram. Soc. Bull., 66, 799-806 (1987)
21. Stevens, R., Zirconia and Zirconia Ceramics, p. 30, 2nd Edition, Magnesium Elektron Ltd., (1986).
22. Buykx, W. J. and Swain, M. W., Advances in Ceramics, Vol. 12: Science and Technology of Zirconia II, 518-527, N. Claussen, M. Ruhle and A. H. Heuer, eds., American Ceramic Society, Columbus, OH (1984)
23. Gorelev, V. I. and Palguev, S. F., Izv. Akad. Nauk. SSSR, Neorg. Mater., 13, 181-182 (1977)